THE JOURNAL OF PHYSICAL CHEMISTRY A

Article

pubs.acs.org/JPCA

Substrate Vibrations as Promoters of Chemical Reactivity on Metal Surfaces

Victoria L. Campbell,[†] Nan Chen,[†,#] Han Guo,[‡] Bret Jackson,[‡] and Arthur L. Utz*[,†]

[†]Department of Chemistry and W. M. Keck Foundation Laboratory for Materials Chemistry Tufts University, Medford, Massachusetts 02155, United States

[‡]Department of Chemistry, University of Massachusetts Amherst, Amherst, Massachusetts 01003, United States

Supporting Information

ABSTRACT: Studies exploring how vibrational energy (E_{vib}) promotes chemical reactivity most often focus on molecular reagents, leaving the role of substrate atom motion in heterogeneous interfacial chemistry underexplored. This combined theoretical and experimental study of methane dissociation on Ni(111) shows that lattice atom motion modulates the reaction barrier height during each surface atom's vibrational period, which leads to a strong variation in the reaction probability (S_0) with surface temperature (T_{surf}). State-resolved beam-surface scattering studies at T_{surf} = 90 K show a sharp threshold in S_0 at translational energy (E_{trans}) = 42 kJ/mol. When E_{trans} decreases from 42 kJ/mol to 34 kJ/mol, S_0 decreases 1000-fold at T_{surf} = 90 K, but only 2-fold at T_{surf} = 475 K. Results highlight the mechanism for this effect, provide benchmarks for DFT calculations, and suggest the potential importance of surface atom induced barrier height modulation in heterogeneously catalyzed reactions, particularly on structurally labile nanoscale particles and defect sites.

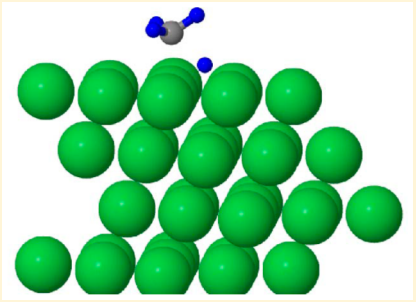

INTRODUCTION

Heterogeneously catalyzed chemical reactions are the foundation of the modern chemical industry. Using a molecular-level understanding of catalysis to improve efficiency, selectivity, and yield is a long-standing goal. Methane dissociation on catalytically active transition metals is a particularly attractive system for study. Its rate-limiting role in the industrial steam reforming reaction provides practical motivation[1] and it is accessible to detailed theoretical and experimental investigation. Over 40 years ago, Polanyi noted that E_{vib} can enhance transition state access and reactivity when the transition state is distorted significantly from the reagents' equilibrium geometry, as is the case for methane's dissociative chemisorption.[2] A series of state-resolved beam-surface scattering studies has now established that methane's vibrational state in the gas phase can dictate the probability and products of its dissociative chemisorption.[3−5] Here, we use experimental and theoretical methods to tackle the less studied but equally important question of how vibrations of atoms in the solid affect heterogeneous chemistry.

Studies of vibrational activation most often focus on gas phase reagents, but the solid surface is also an active participant in heterogeneous gas−surface reactions. Beam-surface scattering experiments have shown that raising T_{surf}, which increases the average E_{vib} of the surface, promotes CH_4 dissociation. Surface temperature effects were most pronounced on Pt(111),[6] Ir(111),[7] and Ru(0001)[8] and less so on Ni(100)[9,10] and Ni(111).[11] In all of these studies, methane molecules possessing a range of E_{vib} were present in the beam, and the resulting vibrational state averaged results muted the impact of T_{surf} on S_0. State-resolved beam-surface scattering experiments eliminate E_{vib} averaging by quantifying S_0 for methane prepared in a specific rotational and vibrational quantum state, and they better isolate and accentuate the impact of T_{surf} on reactivity. Earlier state-resolved studies showed that T_{surf} played a modest role in promoting methane dissociation on Ni(100)[12] and Ni(111)[13] at higher E_{trans}, but the Ni(111) study suggested that T_{surf} effects may be most pronounced at lower E_{trans}. A range of mechanistic origins have been proposed to explain these data. Surface oscillators are a thermal bath available to activate reaction within the context of a statistical model of reactivity.[14] A dynamical hard cube model was invoked to explain the Pt(111) data.[15] Electronic structure calculations reveal that, if the lattice is allowed to relax fully, the metal atom beneath the dissociating methane puckers out of the surface at the transition state.[16−19] Polanyi's rules would then predict that thermal excitation of surface oscillators might provide enhanced transition state access. Electronically non-adiabatic processes could also influence S_0 via their T_{surf} -dependent role in adsorbate−surface energy transfer.[20]

In this study, we use a combination of fully ab initio quantum reaction dynamics calculations and state-resolved beam-surface scattering experiments to understand how substrate vibrations

Special Issue: Dynamics of Molecular Collisions XXV: Fifty Years of Chemical Reaction Dynamics

Received: August 13, 2015
Revised: September 23, 2015
Published: September 25, 2015

DOI: 10.1021/acs.jpca.5b07873
J. Phys. Chem. A 2015, 119, 12434−12441

promote methane's dissociation into chemisorbed CH_3 and H on a Ni(111) surface. Experiments show that surface excitation strongly activates dissociation and, for the first time in a beam-surface scattering experiment, reveal a sharp energetic threshold that permits a direct comparison with Density Functional Theory (DFT) calculations of reaction barrier height. Computational results capture the dramatic surface temperature dependence of reactivity, and they reveal the coupling mechanism that is the basis for activating this gas−surface reaction.

EXPERIMENTAL AND THEORETICAL METHODS

Experiments were performed in a triply differentially pumped supersonic molecular beam surface scattering chamber.[21] Seeded molecular beams of CH_4 in He expanded continuously from a temperature controlled molecular beam nozzle source. A detailed description of the molecular beams we used and their characterization appears Table S1 in the Supporting Information.

To perform quantum-state resolved measurements of methane reactivity, we used light from a continuous wave infrared laser to excite a fraction of the methane molecules in the beam to a select quantum state (J = 2, v = 1 of the ν_3 antisymmetric C−H stretch vibration in this work). The laser intersected the beam in a collision-free region, and excited a fraction of the beam, f_{exc}, ranging from 0.03 to 0.16 depending on the fractional population of the initial state for the infrared transition and the extent to which the transition was saturated. Performing infrared excitation in the collision-free region of the molecular beam ensured that gas-phase collisions did not perturb the laser-excited state as the molecules traveled from excitation region to the surface. Since radiative decay is much slower than the molecules' ca. 200 μs flight time, the laser-excited molecules impinged on the surface in their initially prepared quantum state. The Supporting Information details our determination of f_{exc} for all of the beams used in this study.

After passing through two stages of differential pumping, the methane molecules collided with a temperature-controlled and clean Ni(111) surface. The Ni(111) crystal was polished and aligned within 0.1° of the (111) plane. A combination of Ar ion bombardment, oxidation by O_2, reduction by H_2, and annealing to 1050 K produced a clean surface, as verified by Auger electron spectroscopy (AES). Dose times were adjusted to yield ca. 0.05 ML, and no more than 0.10 ML of C to minimize coverage effects on S_0. At $T_{surf} \geq 90$ K, molecular methane promptly desorbed from the surface, but the methyl product of dissociative chemisorption (or the C atom resulting from its thermal decomposition), were stable up to 600 K.

Following a methane dose, we quantified the chemisorbed products of methane's dissociative chemisorption. We used an isothermal titration method described by Holmblad et al. in their studies of CH_4 dissociation on Ni(100).[9] The method titrates surface-bound C with O_2 and uses the integrated yield of the CO oxidation products to provide a relative measure of the yield of methane's dissociative chemisorption products. We first raised the surface temperature to 550 K, which resulted in dehydrogenation of adsorbed methyl to C, and recombinative desorption of any surface-bound H. Prior studies show that doing so does not lead to loss of C from the surface.[22] We then used our supersonic molecular source held at room temperature to introduce a beam of O_2 into the chamber. An inert beam flag in front of the Ni(111) surface prevented initial reaction of O_2 with C on the surface. We monitored partial pressures at m/z = 16 (O_2), 18 (H_2O), 28 (CO), and 44 (CO_2) with our mass spectrometer. Upon exposure of the surface to the O_2 beam, we observed CO, but no H_2O or CO_2 desorbing from the surface. The integrated CO desorption feature yielded a relative measure of the methane dissociative chemisorption products. Molecular beam reflectivity, Auger electron spectroscopy-based, and bulk H atom titration techniques validated this method. A more detailed description of our method for quantifying reactivity along with figures showing typical data and our calibration curve for C coverage, appears in the Supporting Information.

Measuring S_0 with and without laser excitation allowed us to calculate S_0 for the laser-excited quantum state. We have previously shown that at a given value of E_{trans}, the state-resolved reaction probability, $S_0^{v_3}$, is related to the difference in S_0 for experiments performed with and without laser excitation, $S_0^{LaserOn}$ and $S_0^{LaserOff}$, respectively, f_{exc}, which we report in Table S1, and $S_0^{v=0}$, the reactivity of the v = 0 vibrational ground state, as shown in eq 1.[23]

$$S_0^{v_3} = \frac{S_0^{LaserOn} - S_0^{LaserOff}}{f_{exc}} + S_0^{v=0} \quad (1)$$

We note that $S_0^{LaserOff}$ is always an upper limit on $S_0^{v=0}$, and it most tightly constrains $S_0^{v=0}$ at low T_{nozzle}. For all E_{trans} and T_{surf} reported here, $S_0^{LaserOff}$, and therefore $S_0^{v=0}$, is at least an order of magnitude less than the first term in eq 1, so neglecting $S_0^{v=0}$ results in an error of 10% or less in the reported value of $S_0^{v_3}$.

All electronic structure calculations are performed with the DFT-based Vienna ab initio simulation package (VASP), developed at the Institut für Materialphysik of the Universität Wien.[24−28] Fully nonlocal optimized projector augmented-wave potentials describe interactions between the ionic cores and electrons,[28,29] and we use the Perdew−Burke−Ernzerhof (PBE) functional[30,31] to treat exchange-correlation effects. The metal is modeled as an infinite slab by using a 4-layer 3 × 3 supercell with periodic boundary conditions, corresponding to a methane coverage of 1/9 monolayer. A 13 Å vacuum spacing above the slab separates it from its repeated images.

To construct our potential energy surface (PES), we first locate the minimum energy path (MEP) from reactants to products, passing through the transition state. The distance along this reaction path is s, where $(ds)^2 = \sum_{k=1}^{15}(dx_i)^2$, and the x_i are the mass-weighted Cartesian coordinates of the CH_4 nuclei. At numerous points along this path we compute the total energy, $V_0(s)$. We also perform a normal-mode analysis at these points, which gives us the normal vibrational coordinates Q_k (k = 1−14) and corresponding frequencies $\omega_k(s)$, that describe displacements orthogonal to the reaction path at point s, in the harmonic approximation. Our PES in the reaction path coordinates (s, $\{Q_k\}$), ignoring higher order (anharmonic) terms, is thus

$$V = V_0(s) + \sum_{k=1}^{14} \frac{1}{2}\omega_k{}^2(s)Q_k{}^2 \quad (2)$$

The eigenvectors from our normal mode calculations, $L_{i,k}(s)$, define the transformation between the x_i and our reaction path coordinates:

$$x_i = a_i(s) + \sum_{k=1}^{14} L_{i,k}(s)Q_k \quad (3)$$

DOI: 10.1021/acs.jpca.5b07873
J. Phys. Chem. A 2015, 119, 12434−12441

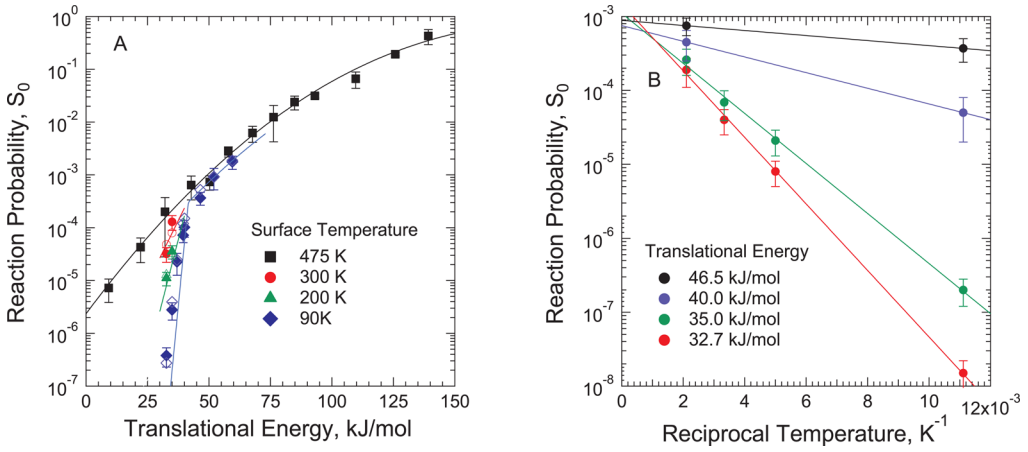

Figure 1. (A) State-resolved S_0 for CH_4 (ν_3, v = 1, J = 2) dissociation on Ni(111) at the indicated T_{surf}. Solid symbols are experimental measurements. Solid lines represent S_0 for molecules with precisely defined E_{trans}. Open symbols are calculated for comparison with the experimental data by convoluting S_0 with each beams' measured E_{trans} distribution. (B) T_{surf} dependence of S_0 at different values of E_{trans}. Solid symbols are deconvoluted values of S_0. Each solid line is a least-squares fit to data obtained at a single value of E_{trans}.

where the $a_i(s)$ give the configuration of the molecule on the reaction path at s. Changing to these reaction path coordinates, our Hamiltonian can be written:[32−34]

$$H = \frac{1}{2}p_s^2 + V_0(s) + H_{vib} - \frac{1}{4}(b_{ss}p_s^2 + 2p_s b_{ss}p_s + p_s^2 b_{ss}) - \frac{1}{2}(p_s\pi_s + \pi_s p_s) \quad (4)$$

where

$$H_{vib} = \sum_{k=1}^{14}\left[\frac{1}{2}P_k^2 + \frac{1}{2}\omega_k^2(s)Q_k^2\right] \quad (5)$$

The momenta conjugate to s and Q_k are p_s and P_k, respectively, and

$$b_{ss} = \sum_{k=1}^{14} Q_k B_{k,15}(s),\ \pi_s = \sum_{k=1}^{14}\sum_{j=1}^{14} Q_k P_j B_{k,j}(s) \quad (6)$$

The vibrationally nonadiabatic couplings are given by

$$B_{k,j}(s) = \sum_{i=1}^{15}\frac{dL_{i,k}}{ds}L_{i,j}(s) \quad (7)$$

To derive eq 4 we have expanded the full Hamiltonian to first order in b_{ss} and π_s. The operator π_s describes energy flow between all modes k and j, through the Coriolis couplings $B_{k,j}$. The operator b_{ss} describes energy flow between the vibrational modes k and motion along the reaction coordinate, due to the curvature, with couplings $B_{k,15}$. The 15th eigenvector is the normalized gradient vector describing motion along the MEP. We have demonstrated that terms higher order in b_{ss} are unimportant.[33−35]

We write the total molecular wave function as

$$\Psi(t) = \sum_{\mathbf{n}}\chi_{\mathbf{n}}(s;t)\Phi_{\mathbf{n}}(\{Q_k\};s) \quad (8)$$

where the $\Phi_{\mathbf{n}}$ are eigenfunctions of H_{vib}, with eigenvalues $\sum_k \hbar\omega_k(s)(n_k+1/2)$. The index $\mathbf{n}$ labels the vibrational state corresponding to the quantum numbers $\{n_k\}$. These vibrationally adiabatic $\Phi_{\mathbf{n}}$ are products of one-dimensional harmonic oscillator eigenfunctions that depend parametrically on s. Given our Ψ, the time-dependent Schrödinger equation gives coupled equations of motion for the wave packets, $\chi_{\mathbf{n}}$, of the form:[33,34,36]

$$i\hbar\frac{\partial\chi_{\mathbf{n}}(s;t)}{\partial t} = \left[\frac{p_s^2}{2} + V_0(s) + \sum_{k=1}^{14}\hbar\omega_k(s)\left(n_k+\frac{1}{2}\right)\right]\times\chi_{\mathbf{n}}(s;t) + \sum_{\mathbf{n}'}\mathbf{F}_{\mathbf{nn}'}\chi_{\mathbf{n}'}(s;t) \quad (9)$$

The wave packets thus evolve on vibrationally adiabatic potential energy surfaces corresponding to each vibrational state $\mathbf{n}$. The operators $\mathbf{F}_{\mathbf{nn}'}$ that couple these states contain matrix elements of the operators b_{ss} and π_s, which describe energy flow between the vibrationally adiabatic states: b_{ss} links states that differ by one vibrational quantum and π_s couples states that differ by two quanta. The $\mathbf{F}_{\mathbf{nn}'}$ also include the operator p_s, which does not commute with the operators π_s and b_{ss}, and the parametric dependence of the $\Phi_{\mathbf{n}}$ on s leads to derivative coupling terms. Our sum over $\mathbf{n}$ in eqs 8 and 9 includes the vibrationally adiabatic ground state, all states with a single vibration excited, and all states with two vibrational quanta excited. Detailed expressions for the equations of motion and the coupling terms can be found in a recent publication.[37] Given some initial vibrational state, $\mathbf{n_0}$, we use standard techniques to evolve the wave packets and energy-analyze the reactive flux.[33,34,36] The result is the rigid-lattice reaction probability, $P_0(E_{trans}, \mathbf{n_0})$.[33,34,36] When the molecule is far above the surface, 5 of the Q_k have zero frequency. These describe molecular rotation as well as X and Y, the location of the molecular center of mass over the surface unit cell. These modes are initially all in the ground state and follow the MEP in the entrance channel. X and Y vary little along the MEP in the entrance channel and up to the TS, with the carbon atom remaining more-or-less over the top site, where the barrier is lowest. The rotation of the molecule in the entrance channel also follows the MEP, and is thus treated adiabatically. As a result, P_0 corresponds to reaction at the top site only, with the assumption of rotationally adiabatic behavior.

To compute the sticking probability S_0 we must average $P_0(E_{trans}, \mathbf{n_0})$ over all impact sites in the surface unit cell, correct for any rotationally nonadiabatic behavior, and include the effects of lattice motion. Motion along X and Y is slow on collision time scales, given the large total molecular mass,

DOI: 10.1021/acs.jpca.5b07873
J. Phys. Chem. A 2015, 119, 12434−12441

typically high E_{trans}, and our normal incidence conditions. We average P_0 over impact sites in the surface unit cell using the following approximation for $P_0(E_i, \mathbf{n}_i; X, Y)$, the reaction probability for impact at a site with coordinates (X,Y):

$$P_0(E_{trans}, n_0; X, Y) \approx P_0(E_{trans} - \Delta V, \mathbf{n}_0) \quad (10)$$

$\Delta V(X,Y)$ is the increase in barrier height relative to the top site, for impact at (X,Y). We compute ΔV from eqs 2 and 3. Any displacement of the molecule along X and/or Y away from the MEP can be written in terms of the coordinates x_i, which define the corresponding displacements Q_k via eq 3. Insertion of these Q_k into eq 2 gives the corresponding increase in V.[36] Recent *ab initio* molecular dynamics studies suggest that the rotational behavior of methane is more sudden than adiabatic.[36,38] We correct our P_0 for this by averaging over all angular orientations of the reactive C−H bond, using an approach similar to that for X and Y.[36] The effects of lattice motion are included as described later in this paper, and in great detail in earlier work.[39,40] The end result is the dissociative sticking probability, S_0.

RESULTS AND DISCUSSION

Reaction probabilities for CH_4 in $v = 1$, $J = 2$ of the ν_3 C−H stretching state (E_{vib} = 36 kJ/mol) were measured at T_{surf} = 90 K, 200 K, and 300 K and compared to prior measurements at T_{surf} = 475 K[41] in Figure 1A. When T_{surf} = 475 K, S_0 increases monotonically and smoothly over the entire E_{trans} range investigated, but at lower T_{surf}, S_0 decreases sharply when E_{trans} falls below 42 kJ/mol. The values of E_{trans} used to plot the experimentally measured S_0 vs E_{trans} (solid symbols in Figure 1A), correspond to the average E_{trans} in the beam, $\langle E_{trans}\rangle$. Our time-of-flight measurements show that the beams are not monoenergetic, but instead have $\Delta E_{trans}/\langle E_{trans}\rangle \approx 5\%$, where ΔE_{trans} is a fwhm. Therefore, the experimental measurements of S_0 are averaged over the spread of E_{trans} in the beam and correspond to $\langle S_0\rangle$. When S_0 is nearly constant over the ΔE_{trans} range, as is the case for T_{surf} = 475 K, the experimentally measured $\langle S_0\rangle$ is very nearly equal to S_0 at the beam's average E_{trans}, and the experimental measurement is an excellent estimate of the inherent value of S_0 at that E_{trans}. When S_0 varies significantly within ΔE_{trans}, as is the case at low T_{surf} and $E_{trans} \leq 42$ kJ/mol, that is no longer the case. The exponential dependence of S_0 on E_{trans} results in molecules with S_0 less than $\langle E_{trans}\rangle$ contributing much less to the algebraic average over ΔE_{trans} than do molecules with E_{trans} greater than $\langle E_{trans}\rangle$. Consequently, $\langle S_0\rangle$ is skewed to a higher value than the inherent S_0 one would measure for molecules with a precisely defined $E_{trans} = \langle E_{trans}\rangle$.

To deconvolute this effect of E_{trans} averaging, we approximate S_0 in the energy threshold region as a simple increasing exponential function whose slope depends on T_{surf}, as shown by the solid lines in Figure 1A. Convoluting this model of S_0 with the measured E_{trans} distribution in each beam results in the open symbols in Figure 1A. We adjusted the slope and intercept of the exponential function to obtain a fit that, when convoluted with the E_{trans} distribution, best describes the experimental data. Therefore, the solid lines in Figure 1A are our best estimates of S_0 for CH_4 (ν_3, $v = 1$, $J = 1$) with a precisely defined E_{trans}. While our simple model likely exaggerates the break in S_0 at E_{trans} = 42 kJ/mol, it does capture the E_{trans} dependence below this threshold, and we use this model as the best representation of S_0 for molecules with a precisely defined E_{trans}.

In Figure 1B, we select four values of E_{trans} and plot $\ln(S_0)$ vs $1/T_{surf}$ to examine how E_{trans} influences the T_{surf} dependence of S_0. We use deconvoluted values of S_0 from Figure 1A to eliminate artifacts from E_{trans} averaging. The plots are linear and yield activation energies of 2.0, 6.5 ± 0.5, and 8.6 ± 0.6 kJ/mol at E_{trans} = 40, 35, and 32.7 kJ/mol, respectively. The data highlight the dramatic role that surface excitation can play in heterogeneously catalyzed reactions. At the lowest E_{trans}, S_0 increases more than 20 000-fold when T_{surf} increases from 90 K to 475 K. Since these E_a values arise from T_{surf} dependence, they provide a measure of how lattice excitation energy promotes reactivity at a fixed E_{trans}.

Computational studies of methane dissociation on Ni, Pt, and Ir surfaces reveal that strong coupling between surface atom displacement and the system's electronic energy explains this striking effect. When the lattice is allowed to relax in TS calculations, the metal atom directly beneath the dissociating methane puckers out of the surface by a few tenths of an Å.[16−19] On Ni(111), the displacement of the nearest-neighbor Ni atoms has only a minimal impact on the TS energy. Figure 2

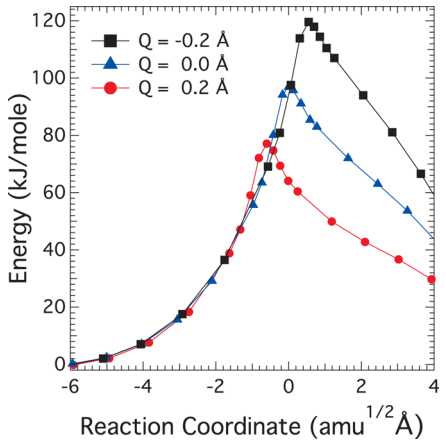

Figure 2. Total energy $V_0(s)$ along the MEP as a function of surface atom displacement, Q. $Q > 0$ corresponds to displacement above the surface plane, while $Q < 0$ describes motion toward the bulk.

shows that the barrier along the MEP *decreases* by nearly 20 kJ/mol when the Ni atom over which the methane dissociates is +0.2 Å above the surface plane, but *increases* by a similar amount when it is 0.2 Å beneath the surface. This effect and the d-band model, which is widely used to predict the impact of *static* lattice strain on reactivity, share a similar origin.[42] Expansive strain weakens metallic bonding, raises the d-band energy, and lowers reaction barriers, while compressive strain raises reaction barriers. In contrast to the d-band model, the mechanism reported here is dynamical; each Ni atom vibration results in a full cycle of barrier height modulation.

How does barrier height modulation explain the E_{trans} dependence shown in Figure 1A? The duration of the methane−surface interaction (≤200 fs) is short relative to lattice vibration (ca. 1 ps).[43] Furthermore, trajectory calculations find that surface atom motion or recoil are relatively minor during the collision, and, at typical collision energies, nearly all reactive trajectories occur over Ni atoms near the outer turning point of their vibrational motion.[40] These observations support treating lattice motion within a sudden approximation. The effective barrier for dissociative chemisorption is highly sensitive to geometric factors including

DOI: 10.1021/acs.jpca.5b07873
J. Phys. Chem. A 2015, 119, 12434−12441

impact site and surface atom displacement, so each incident molecule, with its characteristic molecular orientation, impact site, and collection of vibrational phases, has a corresponding E_{trans} threshold for reaction. When T_{surf} is low, the only molecules with sufficient energy to react at the minimum E_{trans} threshold are those whose incident orientation and impact site are nearly identical to the transition state geometry. Therefore, the value of S_0 at the E_{trans} threshold ($\sim 3 \times 10^{-4}$ at E_{trans} = 42 kJ/mol) is not only state resolved, it is also a surface-site and orientation resolved measure of reaction probability.

We have used DFT to compute how the barrier height changes with lattice motion and at different molecular impact sites in the surface unit cell. In Figure 3, we use the resulting

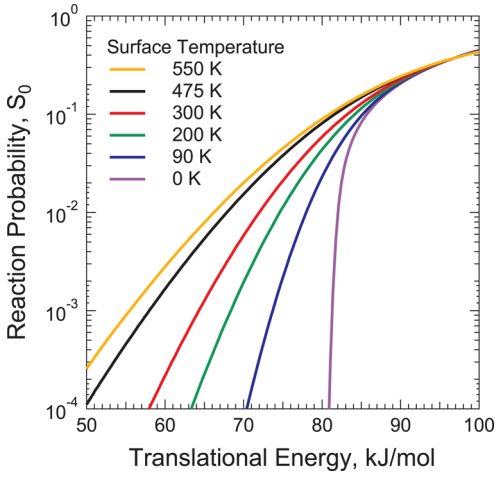

Figure 3. Calculated probability for an incident methane molecule enountering a barrier less than or equal to E_{trans}.

distribution of barrier heights to compute the probability that an incident molecule enounters a barrier less than or equal to E_{trans}. When T_{surf} approaches 0 K, a sharp E_{trans} threshold appears at 82 kJ/mol. As T_{surf} increases, surface motion broadens the distribution by introducing lower ($Q > 0$) and higher ($Q < 0$) barrier reaction paths.

Quantum scattering theory allows a more quantitative analysis of the data. Prior studies accurately described methane dissociation on Ni(100),[33] Ni(111),[34] and Pt(110)-(1 × 2).[44] To incorporate T_{surf} dependence, we address two factors related to lattice motion. First, when the lattice atom vibrates, the location of the barrier in Figure 2 varies with Q by an amount αQ, where α = 0.70. We treated the resulting variation in relative collision velocity similarly to earlier hard cube studies.[15,39,40] Second, the barrier height varies as the Ni atom vibrates; this effect impacts reactivity most.[34] The variation in the barrier height is roughly equal to βQ, where β = 1.16 eV/Å. We treated this effect using a sudden model that averaged over the distribution of surface atom displacements.[39,40] After fully averaging our $P_0(E_{trans}, \mathbf{n_0})$ over surface impact site, angular orientation, and lattice motion, we arrive at the dissociative sticking probability, S_0, plotted in Figure 4. The quantitative agreement between experiment and theory is surprisingly good, particularly considering that the calculations are "ab initio" in the sense that all input to the scattering theory comes from electronic structure calculations, and there are no adjustable or fitted parameters. More importantly, we can relate the observed variation of S_0 with E_{trans} and T_{surf} directly to our PES. We note that a similar comparison with some of this data,

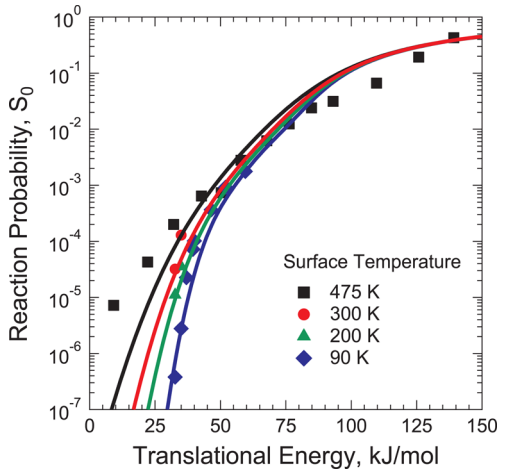

Figure 4. State-resolved reaction probabilities for CH_4 (ν_3, v = 1) dissociation on Ni(111). Solid symbols are experimental measurements and lines are from our scattering calculation.

published in an earlier work,[34] was far less satisfying, and required shifting the computed S_0 along the energy axis in order to better align it with the data. That earlier work was based on DFT calculations using a 2 × 2 supercell. The larger 3 × 3 supercell used in this study eliminates most of the artificial repulsion between methane and its repeated images, resulting in a smaller barrier.

The dissociation barrier height for our 3 × 3 4-layer cell with Q = 0 is 96.9 kJ/mol. Zero-point energy corrections lower this by an additional 15.1 kJ/mol,[19] so, our activation energy is 81.8 kJ/mol. DFT gives E_{vib} = 37 kJ/mol for ν_3, v = 1, so on a rigid metal lattice, our computed S_0 should drop precipitously when E_{trans} drops below 45 kJ/mol ($= E_a - E_{vib}$) and only tunneling can occur. Figure 4 exhibits this behavior at T_{surf} = 90 K. As T_{surf} increases, S_0 increases rapidly for $E_{trans} < 45$ kJ/mol as puckered lattice configurations open new over-the-barrier reaction pathways. Barrier height modulation and the resulting strong dependence of S_0 on T_{surf} may prove to be even more pronounced for undercoordinated atoms at defect sites, or on the surface of structurally labile nanoscale particles. Such atoms are more weakly bound than the Ni atoms in the surface plane of our Ni(111) crystal, and are prone to undergo even larger excursions from their equilibrium position at a given T_{surf}.

The widespread availability of DFT-based electronic structure codes has had a major impact on surface science, but benchmarking these codes is complicated by the lack of exact barrier heights for model systems. A recent approach, which attempts to determine exact barrier heights by fitting exchange-correlation functionals and using a very accurate theoretical treatment of scattering dynamics to reproduce experimental data, works well for H_2 dissociation on Cu(111),[45] but may prove difficult to extend to larger molecules. Figure 1A points to a more general and purely experimental approach to obtaining reaction barrier heights. Given an experimental E_{vib} = 36 kJ/mol for ν_3, v = 1 and an E_{trans} threshold of 42 kJ/mol, experiment yields a barrier height of 78 kJ/mol—surprisingly close to our DFT-PBE value of 81.8 kJ/mol. Increasing our cell size can lower the barrier by an additional kJ/mol or two, so a better estimate of the DFT-PBE zero-coverage activation energy is likely closer to 80 kJ/mol.[18] We note that this agreement is contrary to conventional wisdom: DFT-PBE typically overbinds, leading to barriers that

DOI: 10.1021/acs.jpca.5b07873
J. Phys. Chem. A 2015, 119, 12434−12441

are too low.[38,45] It is hoped that future work will provide an explanation for this.

It is common practice to define a vibrational efficacy in state-resolved S_0 measurements. Very often, the S_0 curve for the vibrationally excited state has the same shape as does S_0 for v = 0, but the excited state curve is shifted to lower energy along the E_{trans} axis. The magnitude of this shift is denoted ΔE_{trans} (a different quantity and unrelated to the E_{trans} that describes the spread of E_{trans} in the beam). It reveals how much less E_{trans} is required to achieve a particular reaction probability given the addition of a known quantity of E_{vib} via state-resolved excitation. The vibrational efficacy, $\eta(v) = \Delta E_{trans}/E_{vib}$ quantifies how effective vibrational excitation is in reducing the E_{trans} threshold for reaction. Efficacies greater than one imply that vibrational energy is more effective than an equivalent amount of translational energy in promoting reaction, as would be predicted by the "late barrier" case of Polanyi's rules for atom−diatom reactivity.

In this work, we seek an analogous expression for vibrational excitation of the lattice. We use the effective activation energies obtained from Figure 1B in the main text as measures of how much lattice excitation is required for reaction at each value of E_{trans}. In Figure 5, we plot those effective activation energies vs

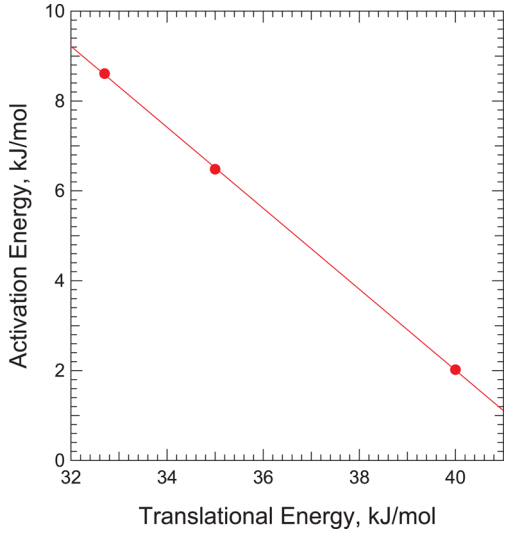

Figure 5. Plot of effective activation energy, as determined from T_{surf} dependence, vs E_{trans}.

E_{trans} for the three values of E_{trans} that are located in the sharp S_0 falloff region of Figure 1A. The plot is linear, and the slope shows how a change in E_{trans} alters the average energy required from vibrational energy of the surface. The reciprocal of the slope corrsponds to $\Delta E_{trans}/\Delta E_{vib}$, a quantity we can compare with vibrational efficacies for the vibrational modes of methane. The plot shows that lattice excitation has an efficacy of η = 1.1 relative to E_{trans} for promoting methane dissociation, which falls between η = 1.25 for the ν_3 C−H stretch and η = 0.4 for the $3\nu_4$ bend on this surface.[5]

One can use quantum dynamics to examine directly how the individual excited states of the lattice oscillator impact reactivity. Unfortunately, to do this we must explicitly treat the lattice motion quantum mechanically along with the molecular degrees of freedom. This can be difficult as large basis sets are required to describe the heavy metal atoms, and many initial oscillator states may need to be considered and averaged over at the experimental substrate temperature. However, we implement such a calculation here for the case of methane initially in the ground state, treating the lattice motion by explicitly including the variable Q in both our wave function and PES. We follow an approach similar to the surface mass model, but modified using our phonon coupling parameters α and β. Specifically, we replace $V_0(s)$ in eq 2 with

$$V_0'(s, Q) = V_0(s + \sqrt{M}\alpha Q) - \beta Q V_0(s + \sqrt{M}\alpha Q)/V_0(0) + V_{lat}(Q) \quad (11)$$

We also replace $\omega_q(s)$ and $\mathbf{F}_{nn'}(s)$ with $\omega_q(s + \sqrt{M}\alpha Q)$ and $\mathbf{F}_{nn'}(s + \sqrt{M}\alpha Q)$, respectively. Thus, the PES and all the couplings shift with Q by an amount $\sqrt{M}\alpha Q$, as in Figure 2. The factor $\sqrt{M}$, where M is the total molecular mass, converts this shift to mass-weighted coordinates. The barrier height also changes by an amount βQ, and this change to the PES is localized about the transition state ($V_0(0)$ is the value at the transition state, and V_0 goes to 0 asymptotically). $V_{lat}(Q)$ is the potential energy for the lattice motion in the absence of the methane. We use a Morse form fit to DFT data for this. Our method of solution is otherwise the same, except that the wavepackets in eqs 8 and 9, $\chi_n(s,Q;t)$, are now two-dimensional.

Figure 6 shows the reactivity curves calculated for the lattice oscillator in each of the first 10 vibrationally excited states.

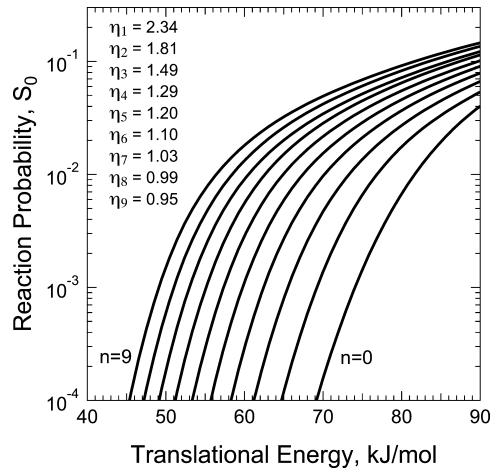

Figure 6. Reactivity curves calculated for the lattice oscillator in one of the first 10 vibrationally excited states. The efficacies, η_n, are listed for the first 9 excited states.

They have been averaged over the impact site as described earlier. Applying the usual approach to calculating vibrational efficacy, the figure shows that the first quantum of surface excitation has an efficacy of η_1 = 2.34, with subsequent excitation providing additional reactivity, albeit with increasingly lower efficacy. The efficacies for the first few excitations of the lattice atom are much larger than what has been observed for molecular vibration for this reaction, underscoring the importance of lattice energy for promoting dissociation. The efficacy decreases to about 1.0 for the eighth quantum. These results are consistent with the experimental measurements, which reflect reactivity averaged over a thermal ensemble of lattice vibrations at the surface temperature.

The dramatic role that lattice vibrations play in modulating surface reactivity may be more common than is currently believed. Early DFT and theoretical studies of dynamics on metals focused on H_2, for which there is very little lattice

DOI: 10.1021/acs.jpca.5b07873
J. Phys. Chem. A 2015, 119, 12434−12441

relaxation upon chemisorption. In contrast, adsorption of the methyl fragment leads to significant lattice puckering.[46] In studies of water dissociation on Cu(111) and Ni(111) we have found similar behavior for the hydroxyl fragment, and the inclusion of lattice motion in recent studies of water dissociation on Ni(111) has led to large variations in S_0 with T_{surf}.[37,47,48]

CONCLUSIONS

Taken together, these results highlight the potentially important role that lattice motion can play in heterogeneous interfacial chemistry. The strong coupling between lattice motion and the system's electronic energy explains how surface vibrations open new over-the-barrier reaction paths for the lower incident energy reagents that dominate thermally activated processes. The appearance of a sharp E_{trans} threshold at low T_{surf} offers a new means of obtaining absolute reaction barrier heights for chemical systems that can be used to benchmark theory. Finally, the strong link between lattice motion and reaction barrier height suggests that engineering structural lability to maximize vibration-induced barrier height modulation may be a fruitful new strategy in catalyst design.

ASSOCIATED CONTENT

Supporting Information

The Supporting Information is available free of charge on the ACS Publications website at DOI: 10.1021/acs.jpca.5b07873.

Additional details on experimental methods including Table S1 and Figures S1 and S2 (PDF)

AUTHOR INFORMATION

Corresponding Author

*E-mail: arthur.utz@tufts.edu. Tel.: 617 623-3473. Fax: 617 627-3443.

Present Address

[#]Department of Chemical Engineering, Massachusetts Institute of Technology, Cambridge, MA, 02139.

Notes

The authors declare no competing financial interest.

ACKNOWLEDGMENTS

V.L.C., N.C., and A.L.U. thank the National Science Foundation for supporting this work through awards CHE-0809802 and CHE-1111702. B.J. and H.G. gratefully acknowledge support from the Division of Chemical Sciences, Office of Basic Energy Sciences, Office of Energy Research, U.S. Department of Energy, under Grant No. DE-FG02-87ER13744.

REFERENCES

(1) J. R. Rostrup-Nielsen, Sehested, J.; Norskov, J. K. In *Advances in Catalysis*; H. Knöpffer, Gates, B. C., Eds.; Academic Press: San Diego, CA, 2002; Vol. *47*, pp 65−139.

(2) Polanyi, J. C. Some Concepts in Reaction Dynamics. *Acc. Chem. Res.* **1972**, *5*, 161−168.

(3) Beck, R. D.; Utz, A. L. In *Dynamics of Gas-Surface Interactions: Atomic-level Understanding of Scattering Processes at Surfaces*; R. D. Muiño, Busnego, H. F., Eds.; Springer-Verlag: Berlin, 2013; Chapter 8.

(4) Utz, A. L. Mode-Selective Chemistry at Surfaces. *Curr. Opin. Solid State Mater. Sci.* **2009**, *13*, 4−12.

(5) Juurlink, L. B. F.; Killelea, D. R.; Utz, A. L. State-Resolved Probes of Methane Dissociation Dynamics. *Prog. Surf. Sci.* **2009**, *84*, 69−134.

(6) Luntz, A. C.; Bethune, D. S. Activation of Methane Dissociation on a Pt(111) Surface. *J. Chem. Phys.* **1989**, *90*, 1274−1280.

(7) Seets, D. C.; Reeves, C. T.; Ferguson, B. A.; Wheeler, M. C.; Mullins, C. B. Dissociative Chemisorption of Methane on Ir(111): Evidence for Direct and Trapping-Mediated Mechanisms. *J. Chem. Phys.* **1997**, *107*, 10229−10241.

(8) Egeberg, R. C.; Ullmann, S.; Alstrup, I.; Mullins, C. B.; Chorkendorff, I. Dissociation of CH_4 on Ni(111) and Ru(0001). *Surf. Sci.* **2002**, *497*, 183−193.

(9) Holmblad, P. M.; Wambach, J.; Chorkendorff, I. Molecular-Beam Study of Dissociative Sticking of Methane On Ni(100). *J. Chem. Phys.* **1995**, *102*, 8255−8263.

(10) Luntz, A. C. CH_4 Dissociation on Ni(100): Comparison of a Direct Dynamical Model to Molecular Beam Experiments. *J. Chem. Phys.* **1995**, *102*, 8264−8269.

(11) Lee, M. B.; Yang, Q. Y.; Ceyer, S. T. Dynamics of the Activated Dissociative Chemisorption of CH_4 and Implication for the Pressure Gap in Catalysis: A Molecular Beam-High Resolution Electron Energy Loss Study. *J. Chem. Phys.* **1987**, *87*, 2724−2741.

(12) Juurlink, L. B. F. *Eigenstate-Resolved Measurements of Methane Dissociation on Ni(100)*; Tufts University: Medford, MA, 2000.

(13) Killelea, D. R.; Campbell, V. L.; Shuman, N. S.; Smith, R. R.; Utz, A. L. Surface Temperature Dependence of Methane Activation on Ni(111). *J. Phys. Chem. C* **2009**, *113*, 20618−20622.

(14) Abbott, H. L.; Bukoski, A.; Harrison, I. Microcanonical unimolecular rate theory at surfaces. II. Vibrational state resolved dissociative chemisorption of methane on Ni(100). *J. Chem. Phys.* **2004**, *121*, 3792−3810.

(15) Luntz, A. C.; Harris, J. CH_4 dissociation on metals: a quantum dynamics model. *Surf. Sci.* **1991**, *258*, 397−426.

(16) Henkelman, G.; Arnaldsson, A.; Jonsson, H. Theoretical Calculations of CH_4 and H_2 Associative Desorption from Ni(111): Could Subsurface Hydrogen Play an Important Role? *J. Chem. Phys.* **2006**, *124*, 044706.

(17) Henkelman, G.; Jónsson, H. Theoretical calculations of dissociative adsorption of CH_4 on an Ir(111) surface. *Phys. Rev. Lett.* **2001**, *86*, 664−667.

(18) Nave, S.; Jackson, B. Methane Dissociation on Ni(111): The Role of Lattice Reconstruction. *Phys. Rev. Lett.* **2007**, *98*, 173003.

(19) Nave, S.; Tiwari, A. K.; Jackson, B. Methane dissociation and adsorption on Ni(111), Pt(111), Ni(100), Pt(100), and Pt(110)-(1 × 2): energetic study. *J. Chem. Phys.* **2010**, *132*, 054705.

(20) Matsiev, D.; et al. On the temperature dependence of electronically non-adiabatic vibrational energy transfer in molecule-surface collisions. *Phys. Chem. Chem. Phys.* **2011**, *13*, 8153−8162.

(21) McCabe, P. R.; Juurlink, L. B. F.; Utz, A. L. A Molecular Beam Apparatus for Eigenstate-Resolved Studies of Gas-Surface Reactivity. *Rev. Sci. Instrum.* **2000**, *71*, 42−53.

(22) Johnson, A. D.; Daley, S. P.; Utz, A. L.; Ceyer, S. T. The Chemistry of Bulk Hydrogen: Reaction of Hydrogen Embedded in Nickel with Adsorbed CH_3. *Science* **1992**, *257*, 223−225.

(23) Juurlink, L. B. F.; McCabe, P. R.; Smith, R. R.; DiCologero, C. L.; Utz, A. L. Eigenstate-Resolved Studies of Gas-Surface Reactivity: CH_4 (ν_3) Dissociation on Ni(100). *Phys. Rev. Lett.* **1999**, *83*, 868−871.

(24) Kresse, G.; Hafner, J. Ab initio Molecular-Dynamics for Liquid-Metals. *Phys. Rev. B: Condens. Matter Mater. Phys.* **1993**, *47*, 558−561.

(25) Kresse, G.; Hafner, J. Ab-Initio Molecular-Dynamics Simulation of the Liquid-Metal Amorphous-Semiconductor Transition in Germanium. *Phys. Rev. B: Condens. Matter Mater. Phys.* **1994**, *49*, 14251−14269.

(26) Kresse, G.; Furthmuller, J. Efficient iterative schemes for ab initio total-energy calculations using a plane-wave basis set. *Phys. Rev. B: Condens. Matter Mater. Phys.* **1996**, *54*, 11169−11186.

(27) Kresse, G.; Furthmuller, J. Efficiency of ab-initio total energy calculations for metals and semiconductors using a plane-wave basis set. *Comput. Mater. Sci.* **1996**, *6*, 15−50.

(28) Kresse, G.; Joubert, D. From ultrasoft pseudopotentials to the projector augmented-wave method. *Phys. Rev. B: Condens. Matter Mater. Phys.* **1999**, *59*, 1758−1775.

DOI: 10.1021/acs.jpca.5b07873
J. Phys. Chem. A 2015, 119, 12434−12441

(29) Blöchl, P. E. Projector Augmented-Wave Method. *Phys. Rev. B: Condens. Matter Mater. Phys.* **1994**, *50*, 17953−17979.
(30) Perdew, J. P.; Burke, K.; Ernzerhof, M. Generalized gradient approximation made simple. *Phys. Rev. Lett.* **1996**, *77*, 3865−3868.
(31) Perdew, J. P.; Burke, K.; Ernzerhof, M. Generalized gradient approximation made simple (vol 77, pg 3865, 1996). *Phys. Rev. Lett.* **1997**, *78*, 1396−1396.
(32) Miller, W. H.; Handy, N. C.; Adams, J. E. Reaction-Path Hamiltonian for Polyatomic-Molecules. *J. Chem. Phys.* **1980**, *72*, 99−112.
(33) Jackson, B.; Nave, S. The dissociative chemisorption of methane on Ni(100): reaction path description of mode-selective chemistry. *J. Chem. Phys.* **2011**, *135*, 114701.
(34) Jackson, B.; Nave, S. The Dissociative Chemisorption of Methane on Ni(111): The effects of Molecular Vibration and Lattice Motion. *J. Chem. Phys.* **2013**, *138*, 174705.
(35) Mastromatteo, M.; Jackson, B. The dissociative chemisorption of methane on Ni(100) and Ni(111): Classical and quantum studies based on the Reaction Path Hamiltonian. *J. Chem. Phys.* **2013**, *139*, 194701.
(36) Jackson, B.; Nattino, F.; Kroes, G. J. Dissociative chemisorption of methane on metal surfaces: tests of dynamical assumptions using quantum models and ab initio molecular dynamics. *J. Chem. Phys.* **2014**, *141*, 054102.
(37) Farjamnia, A.; Jackson, B. The dissociative chemisorption of water on Ni(111): Mode- and bond-selective chemistry on metal surfaces. *J. Chem. Phys.* **2015**, *142*, 234705.
(38) Nattino, F.; Ueta, H.; Chadwick, H.; van Reijzen, M. E.; Beck, R. D.; Jackson, B.; van Hemert, M. C.; Kroes, G. J. Ab Initio molecular dynamics calculations versus quantum state-resolved experiments on CHD3 + Pt(111): New insights into a prototypical gas-surface reaction. *J. Phys. Chem. Lett.* **2014**, *5*, 1294−1299.
(39) Tiwari, A. K.; Nave, S.; Jackson, B. Methane Dissociation on Ni(111): A New Understanding of the Lattice Effect. *Phys. Rev. Lett.* **2009**, *103*, 253201.
(40) Tiwari, A. K.; Nave, S.; Jackson, B. The temperature dependence of methane dissociation on Ni(111) and Pt(111): mixed quantum-classical studies of the lattice response. *J. Chem. Phys.* **2010**, *132*, 134702.
(41) Smith, R. R.; Killelea, D. R.; DelSesto, D. F.; Utz, A. L. Preference for Vibrational Over Translational Energy in a Gas-Surface Reaction. *Science* **2004**, *304*, 992−995.
(42) Mavrikakis, M.; Hammer, B.; Norskov, J. K. Effect of strain on the reactivity of metal surfaces. *Phys. Rev. Lett.* **1998**, *81*, 2819−2822.
(43) Killelea, D. R.; Utz, A. L. On the Origin of Mode- and Bond Selectivity in Vibrationally Mediated Reactions on Surfaces. *Phys. Chem. Chem. Phys.* **2013**, *15*, 20545−20554.
(44) Han, D.; Nave, S.; Jackson, B. The Dissociative Chemisorption of Methane on Pt(110)-(1 × 2): The Effects of Lattice Motion on Reactions at Step Edges. *J. Phys. Chem. A* **2013**, *117*, 8651−8659.
(45) Diaz, C.; et al. Chemically Accurate Simulation of a Prototypical Surface Reaction: H-2 Dissociation on Cu(111). *Science* **2009**, *326*, 832−834.
(46) Nave, S.; Jackson, B. Methane dissociation on Ni(111) and Pt(111): energetic and dynamical studies. *J. Chem. Phys.* **2009**, *130*, 054701.
(47) Hundt, P. M.; Jiang, B.; van Reijzen, M. E.; Guo, H.; Beck, R. D. Vibrationally promoted dissociation of water on Ni(111). *Science* **2014**, *344*, 504−507.
(48) Seenivasan, H.; Tiwari, A. K. Water dissociation on Ni(100) and Ni(111): Effect of surface temperature on reactivity. *J. Chem. Phys.* **2013**, *139*, 174707.

DOI: 10.1021/acs.jpca.5b07873
J. Phys. Chem. A 2015, 119, 12434−12441